Contents lists available at ScienceDirect

Applied Catalysis B: Environmental

Research Paper

Enhancing CO_2 electrolysis to formate on facilely synthesized Bi catalysts at low overpotential

Xia Zhang [a], Tao Lei [a], Yuyu Liu [b,*], Jinli Qiao [a,b,*]

[a] State Key Laboratory for Modification of Chemical Fibers and Polymer Materials, State Environmental Protection Engineering Center for Pollution Treatment and Control in Textile Industry, College of Environmental Science and Engineering, Donghua University, 2999 Ren'min North Road, Shanghai 201620, China
[b] Institute of Sustainable Energy, Shanghai University, 99 Shangda Road, Shanghai 200444, China

ABSTRACT

The electrochemical reduction of CO_2 to fuels and chemicals powered by renewable electricity has been regarded as a promising pathway, which can mitigate the greenhouse effect and energy crisis. However, the development of catalyst with high activity, selectivity, and good stability is still the bottleneck to accomplish this goal. In this communication, we report the promising performance of a micro-structured Bi catalyst which directly converts CO_2 to fuels at room temperature and ambient pressure. The Bi catalyst is designed by a simple and facile aqueous chemical reduction strategy, which readily scales up. The Bi_{45} catalyst exhibits a superior catalytic activity for CO_2 conversion to formate, achieving a high Faradic efficiency of 90% at applied potential −1.45 V vs. SCE. The overpotential for the Bi_{45}/GDE electrode is only 600 mV, a new record to all reported Bi catalysts in the literature. Particularly, the catalyst proves to be robust without any obvious degradation over 20 h of continuous electrolysis at −1.45 V vs. SCE. The notable activity achieved here is ascribed to the special micro-structure of the Bi catalyst, which may afford more active sites, as indicated by comparison to the structure of commercial Bi.

© 2017 Elsevier B.V. All rights reserved.

1. Introduction

With the worsening greenhouse effect and increasing energy crisis, the issue about carbon dioxide (CO_2) utilization and conversion has been attracting tremendous attention [1,2]. To achieve these goals, the electrochemical reduction of CO_2 (ERC) into carbon-based products has been regarded as a potential pathway, because it can perform the carbon-neutral cycle by storing the intermittent renewable energy (i.e., solar, tidal and wind energy) in the CO_2 reduction products [3,4]. However, there are technical limits which have to be overcome, such as the large overpotential due to the thermodynamic stability of CO_2, the low selectivity as a wider products distribution together with the competition of hydrogen evolution. A key technological challenge resides in the development of active electrocatalysts, which are capable of mediating multiple electron and proton transfers, to promote the ERC with high current density at relatively low overpotential, in reactions displaying high selectivity and faradaic yield for a given CO_2 derived product.

Formic acid (HCOOH) or formate ($HCOO^-$) is the favored value-added reduction product owing to the broad application fields, for example, an excellent fuel for direct fuel cells, a useful hydrogen-storage medium, and a most important chemical feedstock [5–7]. Besides, the formic acid produced from CO_2 electroreduction is likely more profitable compared to creating CO, methanol, ethylene and methane [8,9]. The energy-storing reaction and equilibrium potential versus Standard Hydrogen Electrode (SHE) for CO_2 reduction to production formate are as follows (at pH = 7) [10]:

$$CO_2 + 2H^+ + 2e^- = HCOOH, \quad E^\circ = -0.61\,V\,vs.SHE \tag{1}$$
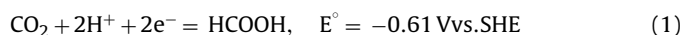
Several heterogeneous catalysts have been particularly assayed to accelerate this reaction in aqueous solution, such as Pb, Hg, In, Sn and Cd. However, only nontoxic and low cost metal Sn has been identified to be a promising catalyst for the conversion of CO_2 to formate [11,12], and many Sn-based catalysts with high Faradaic efficiency for formate (typically >90%) have been reported [10,13,14]. Nevertheless, the low energy efficiency due to the high overpotential impedes the practical application [15]. For example, Meyer et al. loaded the reduced nano-SnO_2 on carbon black and found a Faradaic efficiency for formate (FE_{HCOO^-}) of 86.2% at

* Corresponding author at: College of Environmental Science and Engineering, Donghua University, 2999 Ren'min North Road, Shanghai 201620, China. Institute of Sustainable Energy, Shanghai University, 99 Shangda Road, Shanghai 200444, China.
E-mail addresses: qiaojl@dhu.edu.cn, liuyuyu@shu.edu.cn (J. Qiao).

−1.8 V vs. SCE (Saturated Calomel Electrode), but with the overpotential up to 1.13 V [13]. A high FE_{HCOO^-} of 94.63% was reported on Sn foil, while the electrolysis potential was −2.0 V vs. SCE with high overpotential [16]. Poor stability is another major challenge for Sn-based catalysts to imperatively overcome in final industrial application [7,11]. The life of Sn-based cathode is far lower than the several thousand hours demanded for a practical commercial process [11].

Bismuth (Bi) is a promising metal as a cathode catalysis material for the electrochemical conversion of CO_2, as it is nontoxic and has a low and stable price [17]. In 1995, a FE_{HCOO^-} of 82.7% was reported on Bi shot at high pressure (30 atm) in 0.1 M $KHCO_3$ aqueous solution [18]. The nanostructure Bi catalyst derived from the electrochemical reduction of BiOCl nanosheets (synthesized by hydrothermal method) was reported to have a FE_{HCOO^-} of 92% at −1.5 V vs. SCE, and maintained unchanged for 7 h [19]. Recently, a FE_{HCOO^-} of 91.3% was obtained at Bi electrodeposited on Cu foil electrode at −1.5 V vs. Ag/AgCl with a low overpotential of 0.67 V [20]. Actually, the Bi catalyst exhibits high selectivity for CO_2 reduction to formate, and the overpotential is lower than the Sn-based catalysts. Unfortunately, far less study is conducted on Bi-based catalysts, and there is the need for carrying on obtaining experimental evidence to guide the research efforts for developing and improving these approaches.

In this paper, we show a new design of the direct synthesis of micro-structured Bi catalyst using a facile chemical reduction route in aqueous solution. As illustrated in Fig. 1a, the synthesis route allows easy to realize the large-scale production and high catalytic activity toward CO_2 electroreduction. The obtained Bi_{45} catalyst with micro-structure exhibited high selectivity for formate production with a FE_{HCOO^-} of 90% at −1.45 V vs. SCE in CO_2 saturated 0.5 M $KHCO_3$ aqueous solution. Even more encouraging, this Bi catalyst showed no obvious decay during 20 h continuous electrolysis, indicating the high stability of the catalyst.

2. Bi catalyst synthesis and electrode preparation

The micro-structured Bi catalysts were synthesized by a modified chemical reduction route in aqueous solution [21]. The synthesis procedure was as follows, 2.5 mmol $Bi(NO_3)_3$ $5H_2O$ was slowly added to a three-necked flask containing 10 mL deionized water and appropriate HNO_3. After vigorous stirring for 2 h at room temperature, the mixture was heated to 100 °C, then 30 mL 8.5 mol L^{-1} N_2H_4 H_2O was added into the flask and reacted for 30–60 min at 100 °C. The resulting precipitate was collected by centrifugation and repeatedly washed with absolute ethanol and deionized water for several times to remove the impurities. Finally, the micro-Bi_x (x, the different reaction time) catalysts were obtained after dried in a vacuum oven at 75 °C for 6 h.

For the preparation of Bi_x catalysts coated gas diffusion electrode (GDE), 15 mg as-prepared Bi_x catalysts were dispersed in 4 mL isopropyl alcohol containing 100 mg Nafion® solution (5 wt.%), and then ultrasonicated for 30 min to get a dispersed catalysts ink. The catalysts suspension was coated to a gas diffusion layer (carbon paper, the geometric area is 4 (2 × 2) cm^2) by a spray gun, the final Bi_x catalysts loading was 3 mg cm^{-2}.

3. Results and discussion

3.1. Bi catalyst characterization

Fig. 1f illustrates the XRD patterns of the prepared Bi_{45} catalyst and commercial Bi, which showed the similar characteristic peaks. The peaks at 22.5°, 27.2°, 38.0°, 39.6°, 44.6°, 46.0°, 48.7°, 56.0°, 59.3°, 62.2°, 64.5°, 67.4°, 70.8° and 71.9° are indexed to the (003), (012), (104), (110), (015), (113), (202), (024), (107), (116), (122), (018), (214) and (300) patterns of rhombohedral Bi (JCPDS, 44-1246), respectively, and no other impurity peaks were observed. Among all diffraction peaks of Bi_{45} catalyst, the peak at 27.2° corresponding to the (012) plane is the strongest. These XRD patterns indicate that the Bi^{3+} was completely reduced to Bi^0 under the synthesis condition provided in this work, confirming the high purity of the synthesized Bi_{45} catalyst.

The morphologies of Bi_x catalysts were investigated using SEM images. From Fig. S2a, it can be found that hollow bark-tube-like structured Bi catalyst was formed after 30 min reaction. As the reaction time prolonged to 45 min, the tube-like morphology gradually collapsed and agglomerated together (Fig. 1b). The agglomeration becomes worse as the reaction time increased to 60 min (Fig. S2c). High-magnification SEM micrographs indicated that the three Bi_x samples are all assembled by irregular microstructure Bi sheets with average diameters of 150–250 nm regardless of varying reduction times (Figs. 1 c and S2b, d). By comparison, the commercial Bi was observed to be solid spheres with diameters of 2–4 μm (Fig. S2e). Similar to Bi_x catalysts, the commercial Bi was also aggregated by irregular Bi sheets but more compact, as shown in Fig. S2f.

The TEM analysis further demonstrated that Bi_{45} is composed of irregular sheets, which agglomerate together (Fig. 1d). The lattice fringes could be clearly found with the characteristic spacing of 0.328 and 0.227 nm (Fig. 1e), which match well the (012) and (110) lattice planes of Bi, coinciding with the diffraction peaks in Fig. 1f.

3.2. Electrochemical surface area of Bi catalyst

To estimate the surface area of the Bi catalysts, cyclic voltammetry (CV) was performed in the double layer region of potentials from −0.6 V to −0.8 V vs. SCE at different scan rates in N_2 saturated 0.5 M $KHCO_3$ electrolyte (Fig. S3) [22]. The double layer capacitance values were used to determine the electrochemically active surface area of Bi catalysts. The capacitance is 1.21 mF cm^{-2} for Bi_{45}, which is 2 times larger than that of commercial Bi powder (0.5653 mF cm^{-2}), and the values for Bi_{30} (0.9944 mF cm^{-2}) and Bi_{60} (0.9865 mF cm^{-2}) are both smaller than that of Bi_{45}. This suggests that Bi_{45} can afford larger active surface area than other three catalysts.

3.3. Electrocatalytic reduction of CO_2

Cyclic voltammetry experiments for the prepared and commercial Bi/GDEs were carried out in N_2 or CO_2 saturated 0.5 M $KHCO_3$ electrolyte, with a scan rate of 50 mV s^{-1} and the potential range from −0.6 to −1.7 V vs. SCE (Figs. 2 a and S4a–c). For all Bi/GDEs, the current densities begin to increase at about −1.60 V vs. SCE under N_2 condition, which is caused by the hydrogen evolution reaction (HER). Much larger current responses were observed in CO_2 solution compared to those in N_2 solution, which is ascribed to the electrocatalytic activity of Bi catalysts for CO_2 reduction. The reduction current of 18.9 mA cm^{-2} at −1.7 V vs. SCE was achieved on Bi_{45}/GDE (Fig. 2a), higher than those obtained on Bi_{30}/GDE (15.5 mA cm^{-2}) and Bi_{60}/GDE (16.1 mA cm^{-2}) under CO_2 condition (Fig. S4a–b). This suggests that the aqueous chemical reduction at 100 °C for 45 min is the optimum condition for Bi_x catalysts synthesis. On the contrary, the current density of only 9.1 mA cm^{-2} was observed at −1.7 V vs. SCE on commercial Bi/GDE in CO_2 solution (Fig. S4c), indicating the poorer performance compared to the Bi_{30}, Bi_{45} and Bi_{60} catalysts for CO_2 reduction. Based on the SEM images (Fig. S2e) and electrochemical surface area analysis, the decreased catalytic activity of commercial Bi should be resulted from the solid sphere structure, which may afford fewer active sites than Bi_x catalysts. It should be mentioned that the reduction current
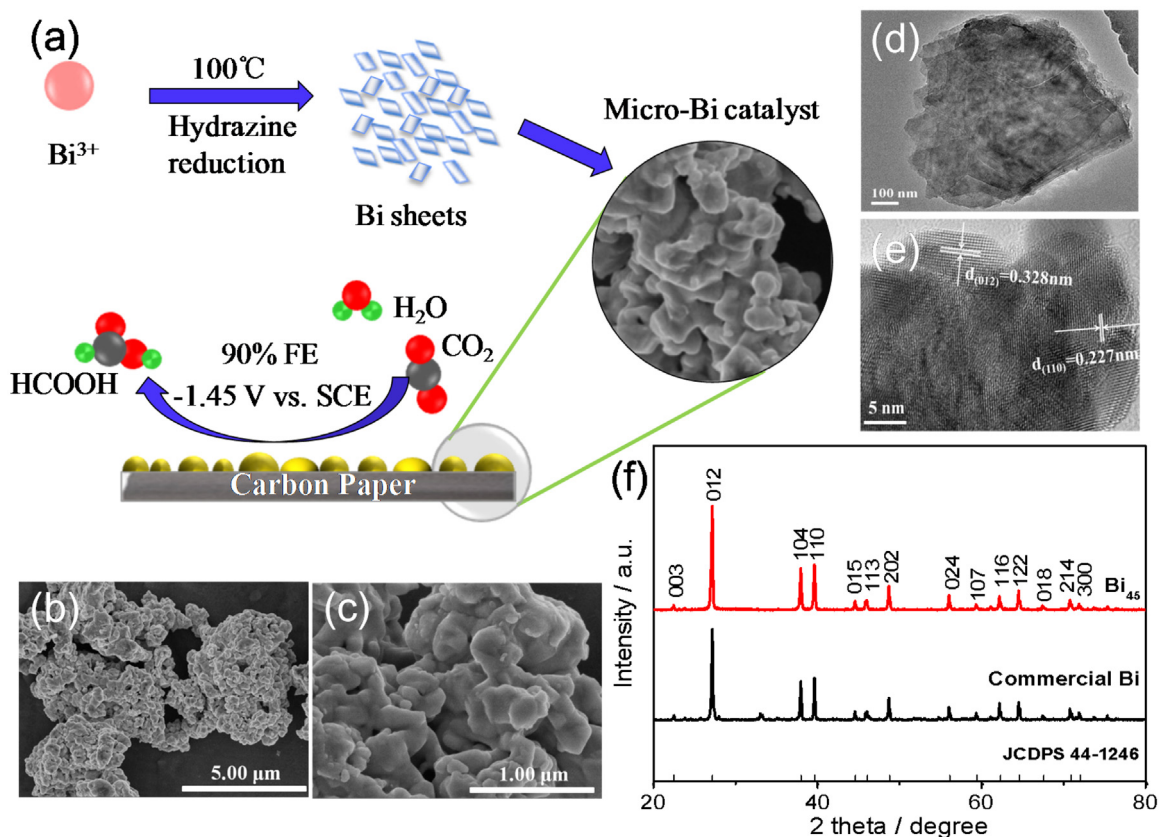
Fig. 1. (a) Illustration of the formation of micro-Bi catalysts for CO_2 electrochemical reduction; (b), (c) SEM images of Bi_{45}; (d) TEM image of Bi_{45}; (e) High-resolution TEM image of Bi_{45}; (f) XRD patterns of commercial Bi powder and Bi_{45}.

of Bi_{45}/GDE was not drastically enhanced compared with Bi_{30}/GDE and Bi_{60}/GDE, due to the similar morphology and structure of the three samples (Figs. 1 c and S2b, d).

The linear scan voltammetry (LSV) was carried out on four Bi/GDEs in CO_2 saturated 0.5 M $KHCO_3$ electrolyte at potential range from -0.6 to -1.7 V vs. SCE with a scan rate of 5 mV s^{-1}. As can be seen from Figs. 2 b and S4d, the Bi_{45}/GDE exhibited the most positive onset potential (about -1.26 V vs. SCE, at a current density of 0.1 mA cm^{-2}) compared to Bi_{30}/GDE (about -1.28 V) and Bi_{60}/GDE (about -1.27 V), which is somewhat more positive than that reported nanostructured Bi (-1.3 V vs. SCE) [19]. These results further indicate that 45 min is the optimum reduction time for Bi_x catalysts synthesis. The commercial Bi gives the most negative onset potential (about -1.35 V vs. SCE, Fig. S4d), which is about 70 mV negative shifts compared to the three Bi_x catalysts, further indicating its poorer electrocatalytic activity towards CO_2 reduction due to the solid sphere structure.

3.4. Catalytic performance for CO_2 reduction to formate

According to the results of CV and LSV experiments, electrolysis test of Bi/GDEs at -1.45 V vs. SCE for 1 h was performed in CO_2 saturated 0.5 M $KHCO_3$ electrolyte, during which CO_2 was continuously bubbled into the cathodic compartment with a rate of 5 mL min^{-1}. The products were analyzed at the end of experiments. At this potential (-1.45 V vs. SCE), formate was the major product and, no CO or H_2 can be detected. As expected (Fig. S5), Bi_{45} catalyst exhibited the highest selectivity for formate compared with Bi_{30}, Bi_{60} and commercial Bi. The FE_{HCOO^-} reaching up to 90% was obtained on Bi_{45}, which is comparable to the values of Bi-based catalysts realized by electroreduction of BiOCl nanosheets (92% at -1.5 V vs. SCE) [19], and the electrodeposition of nanosized bismuth

on copper foil (91.3% at -1.5 V vs. Ag/AgCl) [20], but at a more lower overpotential. Evenly, our catalyst outperformed the nanodendrited Bi in 0.5 M $NaHCO_3$, with a large overpotential nearly 1 V (Table S1). The measured partial current density and corresponding production rate for formate at -1.45 V vs. SCE are -1.5 mA cm^{-2} and 0.5 μmol min^{-1} cm^{-2}, respectively. On Bi_{30} and Bi_{60} catalysts, the FE_{HCOO^-} was decreased to about 80% (Fig. S5). Even this, the value is still higher than those obtained from the reported Sn-based catalysts [12,23,24], further suggesting the good activity and selectivity of the Bi catalysts for CO_2 reduction to formate synthesized in this work.

To further investigate the catalytic activity and selectivity for CO_2 reduction, the controlled potential electrolysis tests of 1 h were performed at Bi_{45} and commercial Bi catalysts. The experiments were carried out in CO_2 saturated 0.5 M $KHCO_3$ electrolyte, and the applied potentials from -1.3 V to -1.6 V vs. SCE (with 0.05 V intervals). As earlier reported Bi-based catalysts[19,22], formate was the major product, and little CO was identified at more negative potential, for example, at -1.5 V, -1.55 V and -1.6 V (Figs. 2 c and S6). From Fig. 2c, for Bi_{45}/GDE, the formate begins to be identified when the electrolysis potential was -1.30 V vs. SCE with a FE_{HCOO^-} of 28%. The highest FE_{HCOO^-} of 90% was obtained at -1.45 V, and then starts to decrease as the electrolysis potential is negatively shifted. At -1.6 V, the FE_{HCOO^-} decreased to 65% ascribe to the enhanced hydrogen evolution, and lots of bubbles are found produced. By comparison, the formate was identified at more negative potential -1.35 V vs. SCE on commercial Bi with a FE_{HCOO^-} of only 8% (Fig. S6). The FE_{HCOO^-} of 65% was obtained at -1.5 V vs. SCE on commercial Bi (Fig. S6), however, the value is much lower than that on Bi_{45} (90% at -1.45 V vs. SCE). Therefore, Bi_{45} showed an enhanced performance for CO_2 electrochemical reduction to formate, which coincides well with the CV and LSV results, suggesting that the morphology and
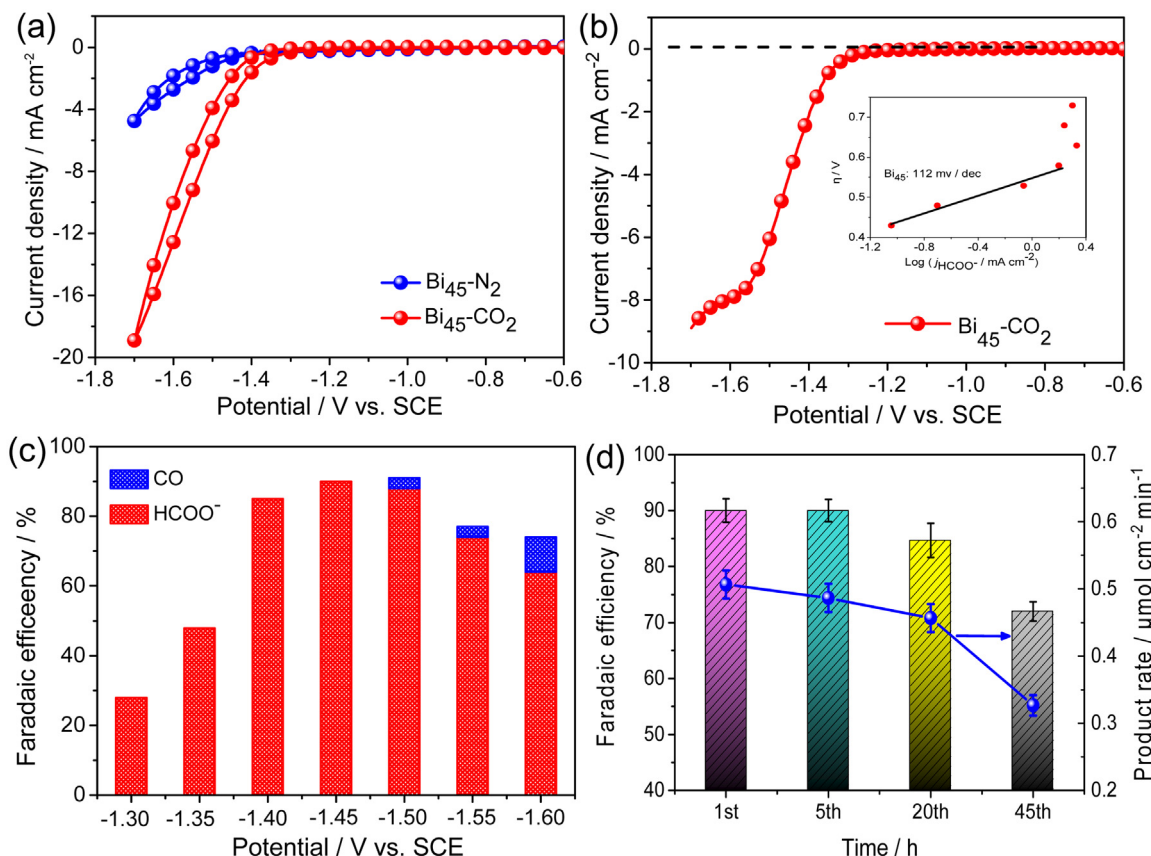
Fig. 2. (a) CV curves of Bi_{45}/GDE in 0.5 M $KHCO_3$ electrolyte saturated by N_2 (blue line) and CO_2 (red line), respectively. The potential range: −0.6 to −1.7 V vs. SCE. Scan rate: 50 mV s^{-1}; (b) LSV curve of Bi_{45}/GDE in CO_2 saturated 0.5 M $KHCO_3$ electrolyte. The potential range: −0.6 to −1.7 V vs. SCE. Scan rate: 5 mV s^{-1}. The inset is Tafel plot for formate on Bi_{45}/GDE; (c) Faradic efficiencies for formate and CO on Bi_{45}/GDE at potential range from −1.3 V to −1.6 V vs. SCE (with 0.05 V intervals) in CO_2 saturated 0.5 M $KHCO_3$ electrolyte. Electrolysis time: 1 h. (d) the stability test of the Bi_{45}/GDE at −1.45 V vs. SCE in CO_2 saturated 0.5 M $KHCO_3$ electrolyte: the Faradaic efficiency and product rate for formate production at various time. (For interpretation of the references to colour in this figure legend, the reader is referred to the web version of this article.)

structure have significant impact on the performance of Bi catalysts in CO_2 reduction.

As further indicated by Faradaic efficiencies in Fig. 2c and Table S1, to get the considerable FE_{HCOO^-}, compared to the Sn-based catalysts, the applied potential for Bi_{45} is obviously more positive. The overpotential for the Bi_{45}/GDE electrode is only 600 mV ($E_{applied}$ = −1.45 V vs. SCE, or −1.21 V vs. SHE), which is the most active one in all reported Bi catalysts in the literature (Table S1). Additionally, the activity of Bi_{45} for CO_2 reduction compares favorably to Sn-based catalysts, which are comparably active but subject to high overpotential.

The mechanistic pathways of CO_2 reduction to formate are varied, which are dependent on the catalyst and the electrolytes. The reduction pathways widely accepted have been proposed that CO_2 reduction involves an initial electron transfer step to form $CO_2^{•-}$ anionic radical, which is regarded as one of the rate-determining steps (RDS), the usual mechanistic pathways for CO_2 reduction to formate are expressed as Eqs. (2)–(4) [25–27]:

$$CO_2 + e^- \rightarrow {}^{•}CO_2{}^-{}_{(ads)} \tag{2}$$

$${}^{•}CO_2{}^-{}_{(ads)} + H^+ \rightarrow {}^{•}COOH_{(ads)} \tag{3}$$

$${}^{•}COOH_{(ads)} + e^- \rightarrow HCO_2{}^- \tag{4}$$

To probe the kinetics of CO_2 reduction, Tafel plot data for CO_2 reduction to formate on Bi_{45}/GDE was conducted by the constant-potential electrolysis. The result is shown in Fig. 2b inset. The Bi_{45} catalyst exhibited a Tafel slope of approximate 112 mV/dec for formate from −0.43 V to −0.58 V overpotentials. This value is closer to 118 mV/dec, which supports the mechanism that a RDS of an

initial electron transfer to CO_2 to form $CO_2^{•-}$ intermediate Eq. (2) [15,28,29]. It has been proposed that the large overpotential during this process ascribes to the intermediate $CO_2^{•-}$ formation that is weakly adsorbed/stabilized to catalyst's surface [30,31].

3.5. Stability of Bi_{45}/GDE for CO_2 reduction

To evaluate the stability of Bi_{45} catalyst, a long-term stability test of 45 h was operated at the potential of −1.45 V vs. SCE. The product of formate was collected and analyzed in the 1st, 5th, 20th and 45th hours, respectively. It can be found from Fig. S7, the total current density was almost unchanged during 20 h of continuous electrolysis. Intriguingly, the FE_{HCOO^-} still remained 87% after 20 h (Fig. 2d), showing negligible change compared to the initial value (90%), and the product rate decreased from 0.51 μmol cm^{-2} min^{-1} to 0.46 μmol cm^{-2} min^{-1}, demonstrating a superior stability of Bi_{45} catalyst for CO_2 reduction reaction in aqueous solutions. After 45 h of continuous electrolysis, the FE_{HCOO^-} declined but still afforded 72%, further proving the excellent stability of the Bi_{45} catalyst. This stable performance differs from the Sn-based catalysts [7,12]. In a continue trickle-bed reactor, Oloman and Li reported that Sn could extend the cathode life to 4 h, after that the formate current efficiency confronted a rapid loss [11]. Agarwal et al. found that the activity of pure Sn and Sn-alloy began to degradation after 20 h polarization in a gas-liquid-solid half cell, after then the Faradaic efficiency suddenly dropped to about 20% [7]. Therefore, the Bi_{45} is a potential catalyst for CO_2 reduction with high selectivity and good stability as well as a simple synthesis route.

4. Conclusions

In this study, we demonstrated an aqueous chemical reduction method for micro-structured Bi catalyst synthesis at moderate temperature, and the process is simple, facile and easy scale-up. The as-prepared Bi catalysts were investigated for CO_2 reduction in 0.5 M $KHCO_3$ aqueous solution, which could activate and convert CO_2 to formate. A maximum FE_{HCOO^-} was achieved up to 90% at −1.45 V vs. SCE on Bi_{45}/GDE with the low overpotential of 600 mV; the potential is the most positive to obtain the comparative FE_{HCOO^-} compared to other reported catalysts. Furthermore, the Bi_{45} catalyst shows stable during 20 h of continuous electrolysis, with negligible loss of FE_{HCOO^-} and current density. Even after 45 h of continuous electrolysis, the FE_{HCOO^-} still affords 72%. Our researches suggest that the achieved micro-structured Bi catalyst would be a potential candidate for catalyzing CO_2 reduction to formate. In recent years, many aspects of catalyst surface modification have been investigated, to improve the efficiency, current density and stability of catalysts in CO_2 reduction. The techniques such as the tailoring of particle size [13], 2D or 3D nanostructure adjustment [12,32,33], porous structure creation [34] and metal-organic framework [35] have been emphasized. We anticipate that the surface modification of Bi catalyst by further efforts, will improve its current density and long-term stability, realizing the industrialization applications of Bi in ERC.

Acknowledgements

Appendix A. Supplementary data

Supplementary data associated with this article can be found, in the online version, at http://dx.doi.org/10.1016/j.apcatb.2017.06.032.

References

[1] J. Qiao, Y. Liu, F. Hong, J. Zhang, Chem. Soc. Rev. 43 (2014) 631–675.
[2] Z. Bitar, A. Fecant, E. Trela-Baudot, S. Chardon-Noblat, D. Pasquier, Appl. Catal. B: Environ. 189 (2016) 172–180.
[3] Q. Lu, F. Jiao, Nano Energy 29 (2016) 439–456.
[4] J. Albo, A. Sáez, J. Solla-Gullón, V. Montiel, A. Irabien, Appl. Catal. B: Environ. 176–177 (2015) 709–717.
[5] X. Yu, P.G. Pickup, J. Power Sources 182 (2008) 124–132.
[6] C. Fellay, N. Yan, P.J. Dyson, G. Laurenczy, J. Chem. Eur. 15 (2009) 3752–3760.
[7] A.S. Agarwal, Y. Zhai, D. Hill, N. Sridhar, ChemSusChem 4 (2011) 1301–1310.
[8] N. Sridhar, D., Hill, DNV Research and Innovation, Position Paper 07-2011.
[9] X. Lu, D.Y.C. Leung, H. Wang, M.K.H. Leung, J. Xuan, ChemElectroChem 1 (2014) 836–849.
[10] J.J. Wu, F.G. Risalvato, F.S. Ke, P.J. Pellechia, X.D. Zhou, J. Electrochem. Soc. 159 (2012) F353–F359.
[11] C. Oloman, H. Li, ChemSusChem 1 (2008) 385–391.
[12] Y. Fu, Y. Li, X. Zhang, Y. Liu, J. Qiao, J. Zhang, D.P. Wilkinson, Appl. Energy 175 (2016) 536–544.
[13] S. Zhang, P. Kang, T.J. Meyer, J. Am. Chem. Soc. 136 (2014) 1734–1737.
[14] C. Zhao, J. Wang, Chem. Eng. J. 293 (2016) 161–170.
[15] Y. Chen, M.W. Kanan, J. Am. Chem. Soc. 134 (2012) 1986–1989.
[16] J.J. Wu, F. Risalvato, X.D. Zhou, ECS Trans. 41 (2012) 49–60.
[17] J.L. DiMeglio, J. Rosenthal, J. Am. Chem. Soc. 135 (2013) 8798–8801.
[18] K. Hara, A. Kudo, T. Sakata, J. Electroanal. Chem. 391 (1995) 141–147.
[19] H. Zhang, Y. Ma, F. Quan, J. Huang, F. Jia, L. Zhang, Electrochem. Commun. 46 (2014) 63–66.
[20] W. Lv, J. Zhou, J. Bei, R. Zhang, L. Wang, Q. Xu, W. Wang, Appl. Surf. Sci. 393 (2017) 191–196.
[21] D. Ma, Y. Zhao, J. Zhao, Y. Li, Y. Lu, D. Zhao, Superlattice Microstruct. 83 (2015) 411–421.
[22] H. Zhong, Y. Qiu, T. Zhang, X. Li, H. Zhang, X. Chen, J. Mater. Chem. A 4 (2016) 13746–13753.
[23] Q. Wang, H. Dong, H. Yu, RSC Adv. 4 (2014) 59970–59976.
[24] Y. Fu, Y. Li, X. Zhang, Y. Liu, X. Zhou, J. Qiao, Chin. J. Catal. 37 (2016) 1081–1088.
[25] W. Paik, T.N. Andersen, H. Eyring, Electrochim. Acta 14 (1969) 1217–1232.
[26] S. Kapusta, N. Hackermant, J. Electrochem. Soc. 130 (1983) 607–613.
[27] R.P.S. Chaplin, A.A. Wragg, J. Appl. Electrochem. 33 (2003) 1107–1123.
[28] C.W. Li, M.W. Kanan, J. Am. Chem. Soc. 134 (2012) 7231–7234.
[29] S. Lee, H. Ju, R. Machunda, S. Uhm, J.K. Lee, H.J. Lee, J. Lee, J. Mater. Chem. A 3 (2015) 3029–3034.
[30] M. Gattrell, N. Gupta, A. Co, J. Electroanal. Chem. 594 (2006) 1–19.
[31] Y. Chen, C.W. Li, M.W. Kanan, J. Am. Chem. Soc. 134 (2012) 19969–19972.
[32] M. Fan, Z. Bai, Q. Zhang, C. Ma, X.-D. Zhou, J. Qiao, RSC Adv. 4 (2014) 44583–44591.
[33] Y.N. Li, J.L. Qiao, X. Zhang, T. Lei, A. Girma, Y.Y. Liu, J.J. Zhang, ChemElectroChem 3 (2016) 1618–1628.
[34] S. Sen, D. Liu, G.T.R. Palmore, ACS Catal. 4 (2014) 3091–3095.
[35] J. Albo, D. Vallejo, G. Beobide, O. Castillo, P. Castano, A. Irabien, ChemSusChem 10 (2017) 1100–1109.